Journal of Experimental Marine Biology and Ecology 471 (2015) 64–76

Contents lists available at ScienceDirect

Journal of Experimental Marine Biology and Ecology

journal homepage: www.elsevier.com/locate/jembe

Ecology of the Ocean Sunfish, *Mola mola*, in the southern California Current System

Tierney M. Thys [a,*], John P. Ryan [b], Heidi Dewar [c], Christopher R. Perle [d], Kady Lyons [e], John O'Sullivan [f], Charles Farwell [f], Michael J. Howard [f], Kevin C. Weng [g], Bertha E. Lavaniegos [h], Gilberto Gaxiola-Castro [h], Luis Erasmo Miranda Bojorquez [h], Elliott L. Hazen [i], Steven J. Bograd [i]

[a] California Academy of Sciences, San Francisco, CA 94118, USA
[b] Monterey Bay Aquarium Research Institute, Moss Landing, CA 95039, USA
[c] NOAA Fisheries, SWFSC, La Jolla, CA 92037, USA
[d] Florida State College, Jacksonville, FL 32256, USA
[e] University of Calgary, Calgary, AB T2N 1N4, Canada
[f] Monterey Bay Aquarium, Monterey, CA 93940, USA
[g] Virginia Institute of Marine Science, Gloucester Point, VA 23062-1346, USA
[h] Centro de Investigación Científica y Educación Superior de Ensenada, Departamento de Oceanografía Biológica, Ensenada, Baja California C.P. 22860, Mexico
[i] Environmental Research Division, Southwest Fisheries Science Center, NOAA Fisheries, Pacific Grove, CA, USA

ARTICLE INFO

Article history:
Received 25 March 2015
Received in revised form 4 May 2015
Accepted 5 May 2015
Available online 29 May 2015

Keywords:
California Current
Fronts
Gelatinous zooplankton
Ocean sunfish
Remote sensing
Satellite tagging

ABSTRACT

The common ocean sunfish, *Mola mola*, occupies a unique position in the eastern Pacific Ocean and the California Current Large Marine Ecosystem (CCLME) as the world's heaviest, most fecund bony fish, and one of the most abundant gelativores. *M. mola* frequently occur as bycatch in fisheries worldwide and comprise the greatest portion of the bycatch in California's large-mesh drift gillnet fishery. In this first long-term tagging study of any ocean sunfish species in the eastern Pacific, 15 *M. mola* (99 cm to 200 cm total length) were tagged in the southern California Bight (SCB) between 2003 and 2010 using 14 satellite pop-off archival tags (PATs) and one Fastloc Mk10 GPS tag. Ten tags provided positional data for a cumulative dataset of 349 tracking days during the months of July through March. Thirteen tags provided temperature and depth data. All *M. mola* remained within ~300 km of the coast, and nearly all exhibited seasonal movement between the SCB and adjacent waters off northern and central Baja California, Mexico. No tagged individuals were tracked north of the SCB. Tag depth data showed diel vertical migration and occasional deep (>500 m) dives. Data from the Fastloc GPS tag allowed close examination of the relationship between the movements of the largest tagged ocean sunfish (2 m TL) and fine-scale oceanographic features. Near-instantaneous satellite sea surface temperature images showed this individual associated with upwelling fronts along its migration path, which exceeded 800 km and ranged from 6 to 128 km from the coast. Tag depth data showed active use of the water column within the frontal zones. Synthetic aperture radar (SAR) images demonstrated that surface slicks, which often indicate convergent circulation, coincided with this type of front. Zooplankton tows in the southern region of tracking off central Baja California, Mexico revealed dense populations of salps toward the warm side of these fronts. Satellite tag and ecosystem data suggest that bio-physical interactions in coastal upwelling fronts create favorable foraging habitat.

1. Introduction

Satellite tracking has allowed new insights into the behavioral ecology of a range of taxa including many marine megafauna such as turtles, whales, seals, fish and squid (Block et al., 2011; Costa et al., 2012). Such studies are providing valuable information for fisheries and the management of ecosystems. One species that has attracted attention, due in part to its diet and unique morphology, is *Mola mola* (Linnaeus, 1758), the common ocean sunfish. Inhabiting all tropical and temperate ocean regions, this species obtains the greatest adult mass of any teleost fish and has the greatest fecundity

* Corresponding author. Tel.: +1 831 277 6763.
E-mail addresses: tierneythys@gmail.com (T.M. Thys), ryjo@mbari.org (J.P. Ryan), Heidi.Dewar@noaa.gov (H. Dewar), chperle@fscj.edu (C.R. Perle), kady.lyons@sbcglobal.net (K. Lyons), JOSullivan@mbayaq.org (J. O'Sullivan), CFarwell@mbayaq.org (C. Farwell), mhoward@mbayaq.org (M.J. Howard), kevinweng@vims.edu (K.C. Weng), berlav@cicese.mx (B.E. Lavaniegos), ggaxiola@cicese.mx (G. Gaxiola-Castro), lmiranda@cicese.edu.mx (L.E. Miranda Bojorquez), Elliott.Hazen@noaa.gov (E.L. Hazen), Steven.Bograd@noaa.gov (S.J. Bograd).

http://dx.doi.org/10.1016/j.jembe.2015.05.005

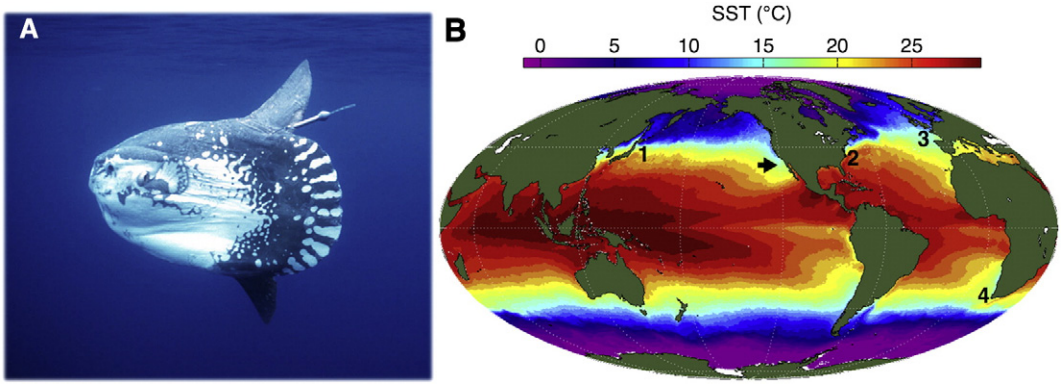

Fig. 1. Tagging studies of ocean sunfish. (A) Photograph of satellite-tagged *Mola mola* off San Diego, California USA. Fish TL = 1.1 m. (B) MODIS Aqua 2013 average sea surface temperature (SST), representing regions in which long-term tagging studies of *M. mola* have occurred, including northwestern Pacific (1) and the northwestern, northeastern and southeastern Atlantic (2–4). The present study in the southern California Current Large Marine Ecosystem (CCLME, arrow) is the first long-term tagging study of *M. mola* in the eastern Pacific. (A) Photo by Mike Johnson, 2006.

(Carwardine, 1995; Roach, 2003; Schmidt, 1921). Beyond their physiological distinctions and unusual shape (Fig. 1A), ocean sunfish are also distinguished by their role in the marine food web. Large ocean sunfish (>1 m total length [TL]) primarily consume gelatinous zooplankton and are the most abundant and largest gelativore in the world ocean (Cardona et al., 2012; Harrod et al., 2013; Nakamura and Sato, 2014).

Ocean sunfish comprise a large percentage of bycatch in gillnet and trawl fisheries worldwide, e.g. 70–95% of total catch in the Mediterranean Sea drift gillnet fishery (DGN) which targets swordfish (genus *Xiphias*) (Silvani et al., 1999; Tudela et al., 2005) and 29–76% of total catch in the South African mid-water trawl fishery, which targets horse mackerel (family Carangidae) (Petersen, 2005; Petersen and McDonell, 2007). In California's DGN fishery, which targets swordfish (*Xiphias gladius*), *M. mola* comprise 14–61% of the total catch (National Oceanic and Atmospheric Administration (NOAA), *unpublished data*). Observers report that most individuals (>95%) are released alive (www.westcoast.fisheries.noaa.gov) although they also note that some fish (an estimated 40% *D. Cartamil*, *pers comm*, Feb 18, 2015) show obvious signs of fishery-induced trauma, including loss of protective mucus, abrasions and bleeding (Cartamil and Lowe, 2004). Post-release survival rate for *M. mola* is unknown in all drift gillnet fisheries. Studies of *M. mola* ecology and behavior are thus motivated by the widespread distribution of the species in vastly different oceanic habitats, its trophic role, reproductive potential and prevalence as bycatch.

M. mola is a seasonal inhabitant in the southern California Current Large Marine Ecosystem (CCLME) (Bass et al., 2005; Cartamil and Lowe, 2004). In contrast to the western Pacific where at least two subspecies have been suggested to occur, *Mola* sp. A and *Mola* sp. B (Sawai et al., 2011; Yoshita et al., 2009), no sub-species of the *Mola* genus have been reported in genetic studies of *M. mola* in the CCLME (Bass et al., 2005). Ocean sunfish have long been residents in this region. Molid fossils from the Miocene have been found along the California coast (Hakel and Stewart, 2002) and archeological sites dating back to 8500 yrs bp suggest a robust prehistoric ocean sunfish fishery once existed along the central and southern California coast (Joslin, 2012; Porcasi and Andrews, 2001). Currently, there are no commercial fishery operations targeting *M. mola* in this region.

The southern CCLME is a comprehensively studied oceanographic region with numerous long-term environmental datasets that are useful for understanding fish movements and behaviors. The longest running extant datasets include the California Cooperative Oceanic Fisheries Investigations (CalCOFI) records of hydrographic and plankton sampling off the California coast and the Investigaciones Mexicanas de la Corriente de California (IMECOCAL) operations off Baja California, Mexico. Recently the CCLME has been forecast to be impacted significantly by ocean acidification (Hofmann et al., 2014) and changing ocean temperatures (NOAA, 2014). This region thus provides an ideal location to investigate the relationships between *M. mola* ecology, oceanographic processes and fishery interactions within the context of broader human impacts.

Previous studies of *M. mola* have yielded valuable insights with regard to natural history, movements and behaviors (Pope et al., 2010). Cartamil and Lowe (2004) investigated short-term (up to 3 days) movements of *M. mola* in the SCB using acoustic tags and continuous manual tracking. This study found that individuals moved a mean distance of 26.8 ± 5.2 km d^{-1} and repeatedly dove below the thermocline during the day. Individuals remained above the thermocline at night and exhibited less overall vertical movement. Long-term (>3 months) pop-up satellite tagging studies of *M. mola* in the northwestern Pacific (Dewar et al., 2010) and 3 regions of the Atlantic (Sims et al., 2009a,b; Potter and Howell, 2011; Fig. 1B) show no evidence of *M. mola* movements across ocean basins, but rather protracted occupation within hemispheric ocean margins. In these studies, latitudinal movement patterns correlated with seasonal changes in temperature and productivity, which likely indicate favorable thermal and foraging habitats (Dewar et al., 2010; Potter et al., 2011; Sims et al., 2009a).

This study examines regional and seasonal movement patterns of *M. mola* tagged between 2003 and 2010. Fastloc GPS data from one tag were integrated with concurrent observations from satellite remote sensing to examine habitat use. These data were coupled with fine-scale ship sampling to explore forage species distributions in relation to habitat. The goal of this study was to provide a greater understanding of *M. mola* ecology, its relationships with oceanographic features and its seasonal movement patterns to help inform fisheries and ecosystem management.

2. Materials and methods

2.1. Tagging and species identification

M. mola were tagged in the SCB from July through October between 2003 and 2010 (Table 1). Fish were tagged either opportunistically during a research longline cruise (n = 4) or during dedicated tagging trips on a small vessel (n = 11). During the dedicated tagging trips, *M. mola* were located from a boat or from a spotter plane (pilot: D. Mauer, Carlsbad, CA, USA) that relayed fish locations via a hand-held radio to crew on a 7 m boat. Free-swimming fish were captured using a 1 m diameter salmon net, and only healthy individuals without obvious wounds or visibly heavy parasite loads were selected for tagging. Individuals were then brought next to the boat, measured to the nearest cm and tagged in the water. A small incision was made below the dorsal fin and a nylon dart, attached to the tags with 300-pound test monofilament line and stainless steel crimps (Fig. 1A), was inserted

Table 1
Tag deployment summary.

PTT Tag type	Tag ID	Deploy Pop-off	Size (cm) Weight (kg)	Deploy Lat (°N) Lon (°W)	Pop off Lat (°N) Lon (°W)	Deployment Duration Tracking days	Distance (km)
41742	03P0266[a]	Sep 6 03	116	32.88	33.55	17[b]	–
PAT		Sep 25 03	82	117.3	118.14		
41749	03P0245[a]	Sep 6 03	117	32.97	32.86	14[b]	49.5
PAT		Sep 25 03	84	117.5	118.11	8	
41752	03P0248	Sep 6 03	143	32.89	32.89	198	55.0
PAT		Mar 21 04	152	117.3	117.91	71	
41756	03P0216	Sep 6 03	150	32.99	26.50	196[b]	–
PAT		Mar 21 04	175	117.5	114.39		
41767	02P0201	Sep 6 03	117	32.91	27.15	198	600.9
PAT		Mar 22 04	84	117.4	116.19	58	
61919	05P0157	Oct 5 06	131	32.92	31.01	174	212.7
PAT		Mar 28 07	117	117.5	117.59	34	
61920	05P0158	Oct 1 06	133	32.85	31.17	181[b]	195.1
PAT		Mar 31 07	123	117.4	116.82		
61922	05P0160	Oct 1 06	130	32.86	29.30	180	445.0
PAT		Mar 30 07	115	117.4	115.22	38	
61924	05P0171	Oct 1 06	131	32.84	30.61	179	256.9
PAT		Mar 29 07	117	117.4	116.91	40	
63978	05P0245	Jul 6 06[c]	92[d]	32.83	28.62	241[b]	530.1
PAT		Mar 04 07		117.8	115.21		
63980	05P0247	Jul 12 06[c]	150	33.12	32.77	240	182.8
PAT		Mar 09 07	175	118.3	120.28	10	
63983	05P0250	Jul 12 06[c]	132	33.12	31.62	240	185.5
PAT		Mar 09 07	120	118.3	117.54	23	
77160	07A0158	Jul 27 07	99	33.19	30.68	181	392.9
PAT		Jan 23 08	51	119.2	116.47	18	
91973	09P0101	Aug 21 09[c]	127	33.40	28.25	90[b]	–
MiniPAT		Nov 19 09	107	118.2	115.06		
89297	10A0564	Aug 28 10	200	32.88	25.90	119	893.9
Fastloc		Dec 25 10	412	117.5	112.84	49	

– insufficient data for track analysis.
Size is total length. Weight is estimated from previously published length/weight relationships (Watanabe and Sato, 2008).
[a] Premature release and presumed mortality.
[b] Insufficient data for tracking or omitted from Fig. 2 for clarity due to shortness of track.
[c] Tags deployed during longline trips.
[d] Pre-caudal length.

with a tag applicator. A pectoral fin clip was taken for genetic analysis before tagged fish were released: all species were later confirmed as *M. mola* using mitochondrial DNA analyses (S. Karl and J. Whitney, *unpublished data*). The entire process was completed in approximately 2–5 min. To ensure proper tag placement and active movements post-tagging, a snorkeler monitored fish visually for up to 5 min. All animals tagged in this manner exhibited strong, healthy swimming movement after tagging with no visible interference from the tag.

During the research cruises, *M. mola* were caught on a longline and pulled into a cradle secured to the boat for tagging. The methods for tag insertion were the same as those used for free-swimming individuals. Following tagging, total length was recorded to the nearest centimeter and a fin clip was taken. The hook was then removed and the fish was released.

Tags deployed included several versions of pop-up satellite tags (PSAT: PAT, mini-PAT, MK10 PAT, MK10-AF PAT [Fastloc GPS], Wildlife Computers, Redmond, WA, U.S.A.) (Fig. 1A; Table 1). The tags were programmed to release after periods ranging from 1 to 9 months. PAT devices collected data on ambient temperature, depth and light intensity (measured as irradiance at 550 nm) every 1–2 min. Fastloc GPS tag collected and archived data every second. Archived PAT data were summarized on-board, and summaries were transmitted after the tag released from the animal. The Fastloc GPS tag data were transmitted along the track and post release.

2.2. Tag horizontal data and analyses

The first 24 h of each track was removed because some degree of behavior modification is expected after tagging (Hoolihan et al., 2011). Tags providing fewer than 7 estimated geolocations were excluded from the horizontal analyses (Table 1). Transmitted data were decoded with Wildlife Computers DAP(R) Processor (www.wildlifecomputers.com). The geolocation routines Trackit (Nielsen and Sibert, 2007) and TrackitSST (Lam et al., 2010), executed in R Statistical Software (R Development Core Team, 2013) using default settings, were used to estimate geolocation. Results from TrackitSST were preferred because this routine combines sea surface temperature (SST) data with a Kalman-filter state space movement model to produce more precise geolocation estimates (Lam et al., 2010; Nielsen et al., 2006). If TrackitSST failed to converge on a resultant track (possibly as a result of unavailable SST data), Trackit was used. The geolocation results of estimated latitudes and longitudes and their associated uncertainties were then imported back into DAP Processor.

The Fastloc GPS electronic tag 89297 transmitted both GPS and Argos quality locations along its track whenever the tag was above the water for a sufficient time interval to turn on. Once data were decoded (as per above), the DAP Processor Fast-GPS solver used Receiver Independent Exchange Format (RINEX) files to post-process transmitted positions to improve accuracy. On days when GPS solutions were not available, Argos positions calculated from >4 uplinks were used to serve as possible along-track substitutes for missing GPS data ($n = 2$).

2.3. Vertical data

Mortalities were excluded from vertical analysis. Mortalities were presumed when depth remained constant for 72 h or when depth exceeded 1500 m, both of which trigger release of the tag. Vertical data were analyzed using transmitted time-at-depth (TAD) and time-

at-temperature (TAT) histograms and profiles of depth and temperature (PDT) data that consisted of 8 temperature and depth measurements over the depth range encountered in a given time interval (Table 2). Data were summarized over programmed time intervals set at 6, 12 and 24 h, depending on the tag. Diel patterns were examined when possible. Tags with bins set at 12 h (n = 3) or 24 h (n = 1) could not exclusively provide day or night intervals, so their data were excluded from diel analysis. Tag 77160 was also excluded since it used an alternate binning scheme. For the 9 tags set at 6 h intervals, the day intervals spanned from 9 am to 3 pm and night from 9 pm to 3 am.

The maximum and minimum temperatures and depths were calculated for each day and night separately and these daily values were averaged for each individual fish (Table 2). Temperature and depth histograms contained 11 to 14 bins based on the binning scheme programmed into the tag. Over the course of the study, tags were deployed with different binning schemes. Due to this inconsistency, histograms were calculated across schemes using methods described in Dewar et al. (2011). For example, temperature bins spread across odd numbers (13–15, 15–17) can be converted to even numbers (12–14, 14–16) by dividing the values for each of the odd bins in half. This provides an estimate for bins of 1 °C width. These bins were then summed accordingly to create common bins. This process assumes that distribution across bins is equal, which may not always be the case, and consequently normalizing in this manner may reduce precision. A separate time series contour plot was made for Fastloc tag 89297 since it provided the highest resolution combination of histogram and location data.

2.4. Satellite remote sensing data and analyses for Fastloc GPS tracking

The high temporal resolution and small error of Fastloc GPS position data (<0.1 km) compared to the fewer positions and larger error (tens to hundreds of kms depending on location class, www.argos-system.org), allowed examination of relationships between an individual fish (tag 89297) and fine-scale ocean features using satellite remote sensing data. These analyses were constrained to the period of August 30 through October 27, 2010, after which the tag provided only one location until its pop-off date of December 25, 2010.

2.4.1. Habitat occupation in relation to sea surface temperature (SST)

Data for examining fish movements in relation to physical oceanography were derived from archived CoastWatch SST (http://coastwatch.pfeg.noaa.gov/erddap/). To increase the potential for matchups between GPS positions and SST images, data from both the Advanced Very High Resolution Radiometer (AVHRR) and the Moderate Resolution Imaging Spectroradiometer (MODIS) Aqua sensor were obtained. AVHRR data prior to application of cloud removal algorithms were examined to ensure that valid SST data were not lost by inaccurate cloud removal. When AVHRR and MODIS images were available for nearly the same time, the image having better coverage of the region occupied by the *M. mola* was selected.

2.4.2. Habitat characterization from synthetic aperture radar (SAR)

SAR data describes ocean surface roughness and can identify features such as slicks, internal waves and other physical phenomena (Apel, 2004; Holt, 2004; Lyzenga et al., 2004). Slicks identified by SAR images can indicate convergent frontal zones (Holt, 2004), and this capability has been useful in coastal plankton ecology research (e.g. Ryan et al., 2005, 2008, 2010). Archived SAR images from the European Space Agency were used to examine the nature of oceanic fronts in regions occupied by the Fastloc tagged fish. The SAR image search was conducted using the EOLI–SA interface (http://earth.esa.int/EOLi/EOLi.html). The only sensor that had acquired SAR images in the region and period of the fish tracking was ENVISAT ASAR. These images had a spatial resolution of approximately 30 m. Although no SAR images could provide coverage exactly when and where the fish was located, two SAR images were matched with SST images to examine fronts detected in the greater study region during the tag deployment period.

2.5. Fine-scale habitat and forage species characterization

In situ oceanographic data were obtained from IMECOCAL cruise IM1010 (October 2010) including data from a profiling CTD with a dissolved oxygen sensor, an underway surface thermosalinograph, and bongo net macrozooplankton collections. Zooplankton displacement volume was measured from the complete sample and functional groups

Table 2
Tag temperature and depth data.

PTT	Bin Interval (h)	SST (°C) range	Min temp ± SD (°C)		Max depth (m)	Min depth ± SD (m)		Max depth ± SD (m)	
			Day	Night		Day	Night	Day	Night
41752	12[a]	16 (13.8–21.0)	10 ± 1.4 (8–14)	11 ± 1.5 (8–15)	336	4 ± 34.1 (0–0)	4 ± 13.8 (0–88)	177 ± 82 (16–300)	80 ± 60.5 (0–292)
41756	12[a]	19 (15.8–23.4)	10 ± 1.5 (8–15)	12 ± 2.6 (9–19)	556	0 ± 4.0 (0–0)	9 ± 20.2 (0–84)	223 ± 80 (0–404)	80 ± 60.5 (0–292)
41767	12[a]	18 (15.0–21.1)	11 ± 1.5 (8–16)	12 ± 2.3 (9–17)	356	2 ± 8.8 (0–0)	3 ± 14.9 (0–56)	209 ± 75 (16–308)	121 ± 87.7 (0–248)
61919	6	16 (14–19)	10 ± 1.5 (8–14)	15 ± 1.5 (12–17)	316	13 ± 60.1 (0–8)	4 ± 7.0 (0–8)	182 ± 117 (0–316)	30 ± 18.6 (0–88)
61920	6	15 (12–18)	10 ± 0.6 (9–11)	13 ± 1.3 (11–14)	360	49 ± 116 (0–0)	2 ± 2.2 (0–4)	203 ± 76 (88–268)	42 ± 37.9 (0–100)
61922	6	17 (15–23)	11 ± 2.1 (8–16)	15 ± 1.7 (12–16)	512	20 ± 51.5 (0–0)	2 ± 4.0 (0–8)	168 ± 94 (0–284)	31 ± 21.0 (0–76)
61924	6	18 (14–23)	10 ± 1.7 (9–13)	14 ± 2.4 (12–17)	400	15 ± 36.1 (0–96)	2 ± 3.1 (0–8)	173 ± 119 (0–292)	25 ± 14.2 (4–48)
63978	6	18 (18–23)	12 ± 2.3 (16–19)	14 ± 1.3 (12–16)	312	1 ± 3.6 (0–0)	8 ± 20.7 (0–68)	96 ± 89 (0–296)	66 ± 26.9 (24–104)
63980	6	21 (20–21)	11 ± 2.8 (9–13)	12 ± 0.4 (12–13)	336	0 ± 0 (0–0)	0 ± 0 (0–0)	100 ± 141 (0–200)	30 ± 8.5 (24–36)
63983	6	18 (7–24)	10 ± 1.0 (9–13)	13 ± 2.1 (8–16)	396	10 ± 37.1 (0–0)	3 ± 6.7 (0–0)	208 ± 81 0–320	36 ± 32.9 0–144
77160	6[a]	19 (14–20)	9 ± 0.9 (8–11)	14 ± 2.1 (11–20)	504	1 ± 6.1 (0–0)	1 ± 2.2 (0–8)	209 ± 61 (72–273)	36 ± 16.2 (16–64)
89297	6	19 (16–22)	12 ± 3.2 (0–18)	14 ± 2.4 (7–19)	520	23 ± 22.2 (0–88)	9 ± 9.2 (0–40)	139 ± 84.6 (0–520)	73 ± 73 (16–520)
91973	24[a]	21 (20–24)	–	–	312	–	–	–	–

[a] Not included in Fig. 3 due to bin incompatibility.

were counted from a fraction (1/8) of selected samples. Collection methodologies are described in Lavaniegos et al. (2002) with the one exception being that macrozooplankton for cruise IM1010 were collected with a 71 cm instead of a 61 cm diameter bongo net.

3. Results and discussion

3.1. Tag and geolocation performance

Thirteen out of the 15 tags remained attached for their set deployments with durations ranging from 90 to 241 days (Table 1). The two tags that released prematurely, 41742 (17 days) and 41749 (14 days), indicated fish mortality. Tag 41742 was retrieved and its data revealed it remained at 76–80 m for 3 days before releasing. Tag 41749 sank to a depth >980 m, released and initiated transmission at the surface after 3 days. The fact that both these animals died within similar periods following release suggests that tagging may have been a possible cause of death. With additional tagging and a large enough sample size, it may be feasible to estimate mortality within this population as has been suggested by previous studies on marine turtles (Hays et al., 2003). Tags 41756, 61920, 63978 and 91973 did not provide sufficient geolocation data for track analysis.

A total of 313 geolocation tracking days were obtained from all tags. From the 119 day track of the Fastloc GPS tagged fish (89297), 83 days provided 49 daily positions, and two additional days were supplemented with Argos positions. Positional uncertainty (mean ± SD) for longitudes using TrackitSST (29.1 ± 6.2 km) was similar to that for Trackit (29.3 ± 9.8 km), while for latitudes, TrackitSST (49.5 ± 12.5 km) yielded slightly increased precision over Trackit (52.7 ± 16.3 km). For all other tags, an average of 23% (median 20%) of the total possible tracking days resulted in 313 total geolocations with estimates of uncertainty provided by TrackitSST (n = 4 tags, 86 days) or Trackit (n = 8 tags, 227 days) methods.

3.2. Geographic movements

Examination of *M. mola* geographic movement was constrained to the 9 tag deployments where fish survived and provided tracks of sufficient duration and temporal resolution (Table 2, Fig. 2). No tagged individuals moved north of the SCB. All *M. mola* were tracked southward into Mexican waters (Fig. 2A). Most fish (7 out of the 9) were in Mexican waters by October, and most of these did not return to US waters until February of the following year (Fig. 2A, B). All fish remained within 300 km of the shore with the majority of residence within 100 km of shore (Fig. 2A). Four fish exhibited southward migrations extending

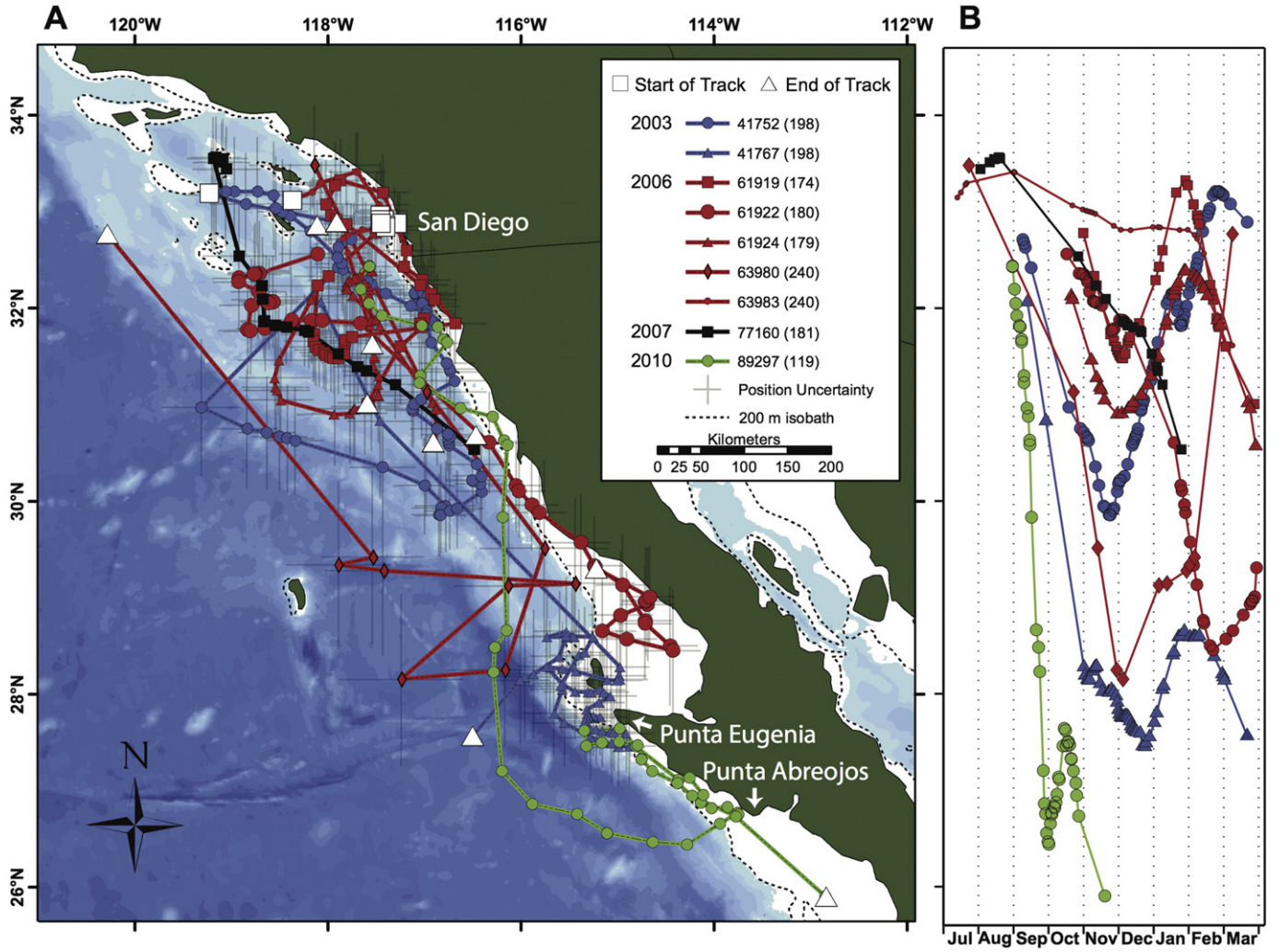

Fig. 2. Geographic and seasonal movements of ocean sunfish. (A) Horizontal movements of *M. mola* determined from satellite tracking. Estimates of daily positions are shown for each of the 9 *M. mola*. Symbols indicate individual fish locations; the color of symbols and connecting lines indicates year of deployment. Positional uncertainty estimates are represented by gray bars in latitude and longitude at each position. Positional certainty is much higher for tag 89297 (Fastloc GPS, green circles over green line). Background is the GEBCO_2013 global bathymetric grid at 30 arc sec intervals. In the legend, the deployment duration in days is indicated in parentheses after the Tag ID number. (B) Latitudinal position of *M. mola* from (A) represented relative to day-of-year.

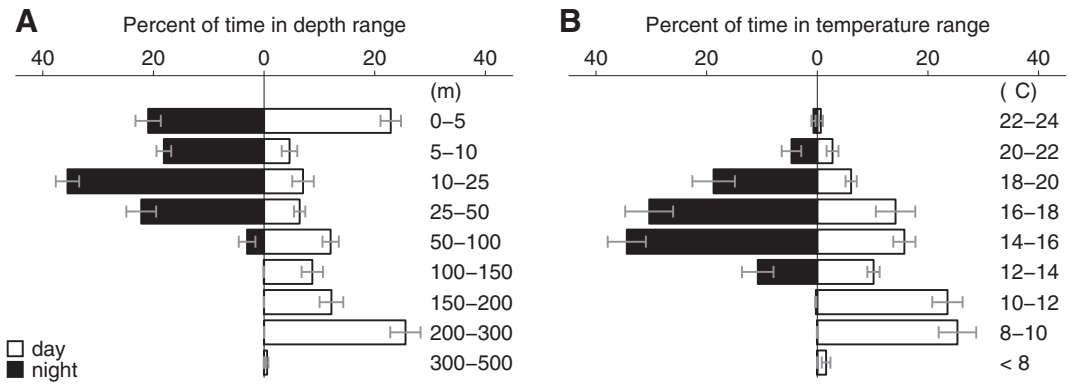

Fig. 3. Depth and temperature range occupation of ocean sunfish. (A) Depth and (B) temperature histograms for day (white) and night (black) averaged for all fish in Table 2, except those with 12 and 24 h binning schemes and tag 77160, which used an alternate binning scheme. Data represent average percent time spent within each binned range.

further than the others (tags 41767, 61922, 63980 and 89297). The farthest and most rapid southward migration (~670 km in one month) was by the largest fish (tag 89297, 2 m TL), which was tracked as far south as Punta Abreojos, Baja California Sur. The extent and timing of southward and northward movements were variable (Fig. 2B). However, 6 out of the 8 tags with records >4 months, reversed their southward movements to northward during the late fall and winter months of November–December (Fig. 2B).

Horizontal movements were similar to those documented for other *M. mola* long-term tagging studies: individuals tagged in coastal regions did not cross ocean basins but persistently inhabited the margins of their respective ocean basins (Dewar et al., 2010; Hays et al., 2009; Nakamura et al., 2015; Potter et al., 2011; Sims et al., 2009a,b). Past studies report *M. mola* alternating between movement toward or away from the equator, presumably to take advantage of greater productivity in spring and summer at higher latitudes (Parsons et al., 1984). For example, between spring and fall 2006, an ocean sunfish migrated 2619 km northeastward from coastal Japanese waters along the northwest Pacific margin (Dewar et al., 2010). *M. mola* may also migrate to avoid cooler water temperatures. For example, as temperatures cooled between fall and winter 2005, an ocean sunfish migrated 2520 km from New England waters southward into much warmer waters around the Bahamas (Potter et al., 2011). A combination of productivity and temperature likely drives these seasonal migrations.

3.3. Southern CCLME depth and temperature preferences

M. mola occupied different depth and temperature ranges during the day versus night (Table 2, Fig. 3). This pattern is consistent with diel vertical migrations (DVM), examples of which are presented for the Fastloc GPS tag in Section 3.4. During the day, individuals frequented deeper, cooler waters with 59% of occupancy below 50 m. During the night, they were in shallower, warmer water with 97% of occupancy in the upper 50 m. Average maximum nighttime depth across all fish was 59 ± 9 m (SE) compared to 174 ± 8 m during the day. Correspondingly, the average minimum nighttime temperature was 13 ± 0.2 °C (SE) compared to 11 ± 0.2 °C during the day. Occasional deep dives (>500 m) were recorded for 4 *M. mola*, extending into temperatures as cold as 6.6 °C (Table 2). Deep dives could be due to a variety of factors as suggested by Houghton et al. (2008), including predator and ship evasion, thermoregulation and searching for prey. Ship evasion response could be explored in future studies by comparing deep dive locations with geospatially matched automatic identification system (AIS) data collected by vessel traffic services (VTC) to identify and locate vessels. More detailed dive profile data than what was available in this study is needed to explore any additional hypotheses.

Reasons underlying routine vertical movement have been linked to several factors. Vertical movement is likely used as a foraging strategy in search of patchily distributed prey as well as targeting the migration

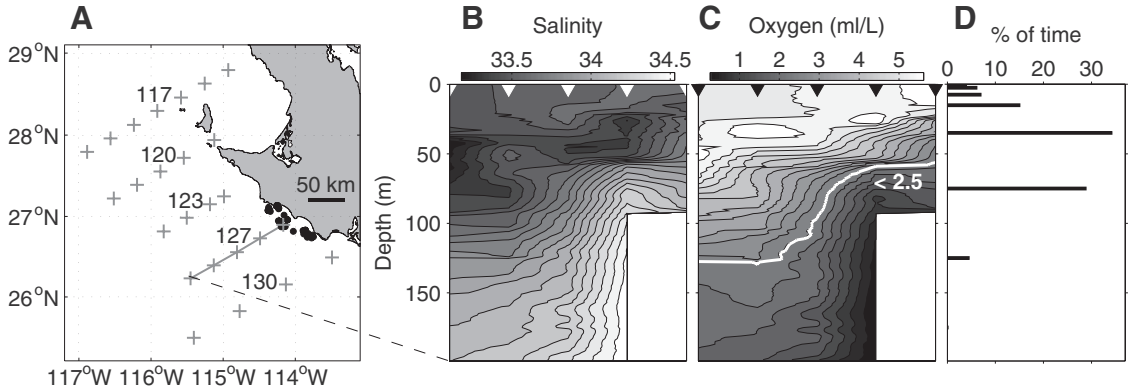

Fig. 4. Ocean sunfish depth occupation in relation to oxygen distributions. (A) Map of station locations occupied during IMECOCAL cruise IM1010, October 12–17, 2010. The gray line highlights Line 127, which approached the coast within close range of the *M. mola* migration path (solid black circles). (B, C) Line 127 sections of salinity and dissolved oxygen concentration, acquired between October 15, 10:00 and October 16, 03:00. The most inshore station was on the shelf (92 m). (D) Depth occupancy of the *M. mola* near the most inshore station during northward migration (October 3, 15:00–October 10, 17:00) and southward migration (October 24, 23:00–October 27, 14:00).

of the deep scattering layer (DSL) (Cartamil and Lowe, 2004; Dewar et al., 2010; Potter and Howell, 2011; Sims et al., 2009a,b). The bimodal depth distribution during the day (Fig. 3) is consistent with repetitive dives between the mixed layer and the DSL. In Japanese waters, Nakamura et al. (2015) show *M. mola* surface to warm-up following dives below the thermocline to the colder deep scattering layer.

Cartamil and Lowe (2004) also suggest that individuals in the SCB may be recovering after frequenting depths with decreased oxygen concentrations. Ocean hypoxic zones (oxygen levels <2.5 ml l^{-1}) are thought to induce avoidance responses in many fishes (Brill, 1994; Davis, 1975; Dewar et al., 2011). Over the past 30 years throughout the CCLME, the hypoxic boundary appears to be shoaling (Bograd et al., 2008). In this study, a cross-shelf section from the 2010 IMECOCAL cruise approached, in space and time, the GPS tracked *M. mola* and thus allowed examination of potential impacts of dissolved oxygen concentrations on *M. mola* vertical movements (Fig. 4A). Due to coastal upwelling, salinity and oxygen isopleths shoaled toward the coast (Fig. 4B, C). Low oxygen levels (<2.5 ml l^{-1}) were recorded <60 m below the surface at the most inshore station (Fig. 4C), and the water column structure suggests that these low oxygen waters may have been even shallower closer to the coast. When the tagged individual was in the region of the inshore station, it spent 34% of its time below the shallow limit of the low oxygen detected during the Line 127 survey (<2.5 ml l^{-1}, Fig. 4D). These findings suggest that *M. mola* may be able to tolerate low oxygen levels. Additional investigations into physiological tolerances of this species would be interesting, particularly in light of recent reports of ocean oxygen minima expanding both in the SCB and globally as a result of climate change (McClatchie et al., 2010; Stramma et al., 2010).

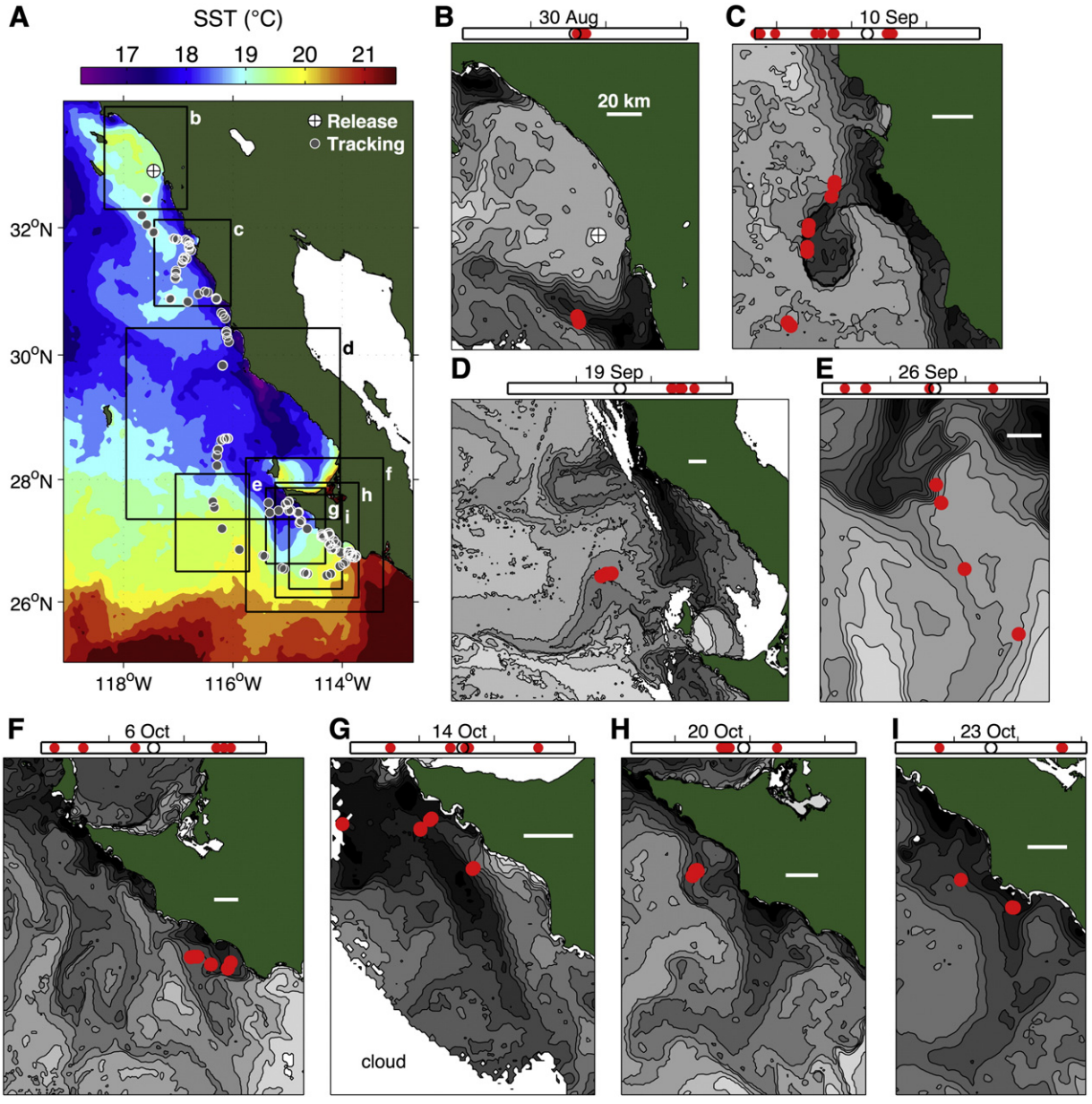

Fig. 5. Consistent association of a large sunfish (2 m total length) with upwelling fronts. (A) Mean sea surface temperature (SST) during August 30 through October 27, 2010, corresponding with the period of tracking shown for Fastloc tag 89297. Boxes identify individual synoptic SST image domains. (B–I) SST images from the domains labeled in (A). All images are nearly instantaneous, except for (C), which is a 1-day composite. Images B, C, F and H are from AVHRR; images D, E, G, and I are from MODIS Aqua. In each image, gray scale shading is adapted to the range of variation within the domain; darker shades represent relatively cold water associated with coastal upwelling. White scale bars in all images are 20 km. *M. mola* positions (red circles) are shown for available tracking data within ±1.5 days of each image acquisition time. In the time reference atop each image, position times (solid red circles) are shown relative to image time (open black circle) during a 3-day window centered on the image time.

3.4. Ecological insights from GPS tracking and ecosystem data

The high accuracy of the Fastloc GPS tag, 89297, coupled with the oceanographic and prey data, allowed closer examination of relationships between the largest of the tagged *M. mola* and the ecosystem. During late August to late October 2010, GPS tracking provided excellent temporal resolution as this sunfish traveled more than 800 km along a meandering trajectory from its release location off San Diego, California, to as far south as Punta Abreojos, Baja California, México (26.5°N, Fig. 2). For approximately half of this period, the individual remained close to the coast within a relatively small region off Baja California, south of Punta Eugenia (Fig. 2, between ~26.5°N and 27.7°N). It approached the southern end of this region from offshore and then migrated first northward then southward along that portion of the coast during October. This region was also occupied by the only other *M. mola* that was tracked this far south in 2003 (Fig. 2, tag 41767). Although the positional accuracy of tag 41767 is much less than that of tag 89297, the many consistent geolocations from tag 41767 in this region lend confidence to the interpretation of overlap in the geographic occupation of these sunfish. Results suggest that the area off Punta Eugenia might be an ecologically important destination for *M. mola* in the southern CCLME and worthy of further investigation. Adjacent southern waters have been identified as a hotspot for numerous marine animals including several species of tuna, sharks, whales, sea turtles and seabirds (Etnoyer et al., 2006; Peckham et al., 2007; Schaefer et al., 2007; Wingfield et al., 2011; Wolf et al., 2009).

3.4.1. Association with fronts

Eight spatiotemporal matchups between GPS positions and satellite SST (described in Section 2.4.1) were possible. All matchups showed sunfish 89297 occupying a specific type of front that develops along the periphery of cold water generated by coastal upwelling (Fig. 5). Although the front was associated with upwelled water in each (Fig. 5B–I), the specifics of the frontal structures were variable. The first two cases showed association of the sunfish with relatively sharp frontal gradients close to the coast (Fig. 5B, C). The next two cases showed association with weaker fronts further offshore (Fig. 5D, E). The warmer temperatures and weaker frontal gradients of the filament offshore are consistent with warming during offshore transport, due to mixing and solar heating. The last 4 cases, in the region between Punta Eugenia and Punta Abreojos during October, again showed association with relatively sharp nearshore fronts (Fig. 5F–I). These findings suggest that frontal systems play a central role in *M. mola* habitat in the southern CCLME. Previous studies using a variety of techniques and datasets have indicated associations of *M. mola* with different types of fronts (Potter et al., 2011; Sims and Southall, 2002). The present study, however, is the first to match Fastloc GPS position data with near-instantaneous views of SST to reveal consistent occupancy of frontal habitats.

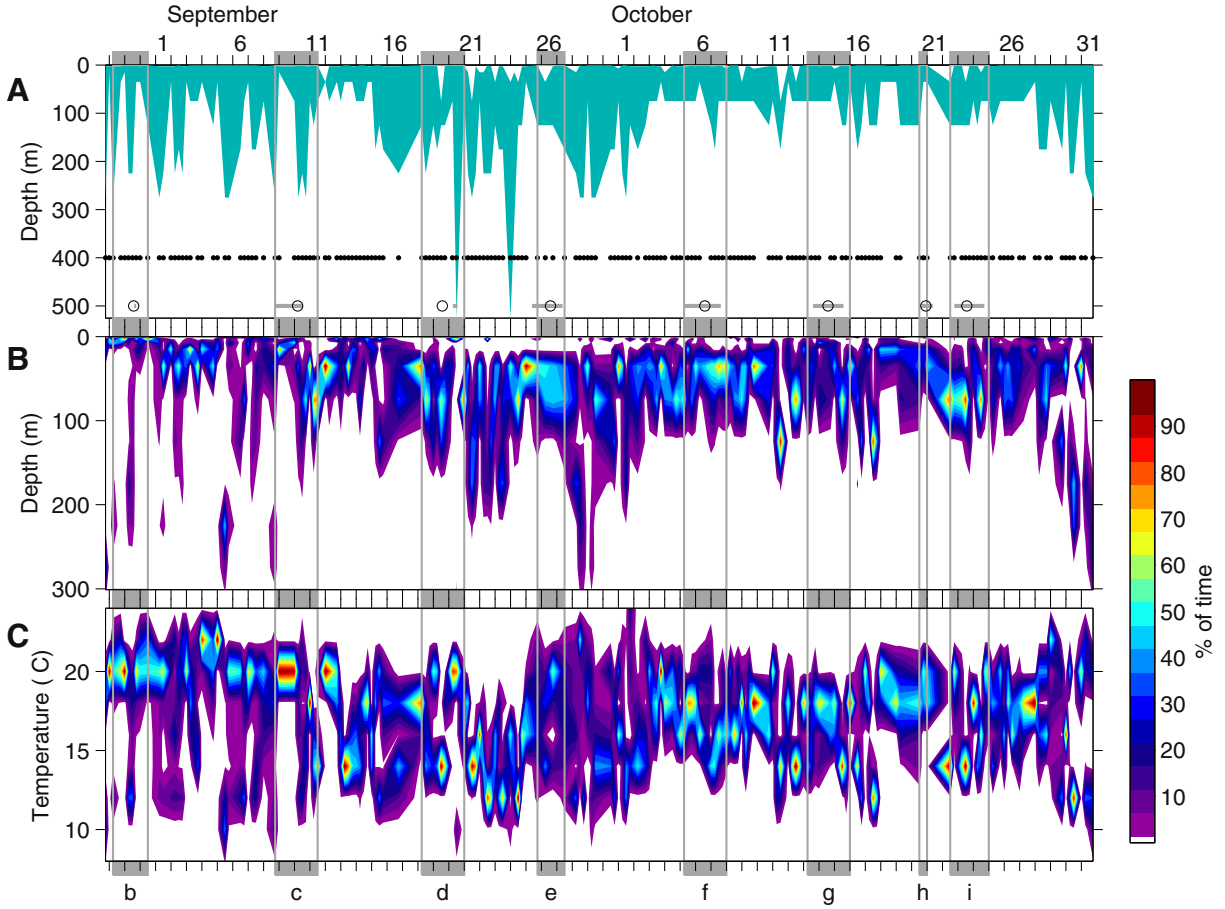

Fig. 6. Depth and temperature occupation of tag 89297. Time-series contour plots represent the migration between San Diego, California and Mid-Baja California, Mexico for (A) depth envelope, (B) depth distribution, and (C) temperature distribution. The depth range in (B) is constrained relative to (A) to show detail of where the fish spent most of the time. Time reference is local, and tic marks for each day indicate midnight. Solid black circles at 400 m in (A) show the times for which statistical summaries within a 6-hour interval were received from the tag. In (B, C) depth and temperature axes represent the midpoint of a bin, and color represents the percent of time the fish spent in a depth or temperature bin within a 6-hour interval. Periods boxed in gray define the times during which tag summary data were available within ±1.5 days of a satellite SST image (Fig. 5). The open black circles at 500 m in (A) identify the times of the satellite images shown in Fig. 5; lower case labels at the bottom of (C) correspond to domain labels in Fig. 5A. The gray horizontal lines at 500 m in (A) define the time windows of Fastloc GPS coverage shown in each of the synoptic images in Fig. 5.

Table 3
Depth occupation in coincidence with frontal zones for *M. mola* tag 89297. Image ID letters correspond with image panels in Fig. 5. Time and depth range data are based on available data within ±1.5 days of each image time (gray boxes in Fig. 6).

Case study	B	C	D	E	F	G	H	I
Time (h)	54	66	66	42	66	66	12	60
Depth range (m)	0–275	0–275	0–520	0–175	0–175	0–125	0–125	0–125

Frontal systems are highly variable in spatial scale, duration and physico-chemical and biological factors, and their effects extend across trophic levels (Belkin et al., 2014). Within the CCLME, aggregating and foraging behaviors around fronts have been observed for a variety of species including tuna (Fiedler and Bernard, 1987), cetaceans (Tynan et al., 2005) and leatherback turtles (Benson et al., 2007). Recently, studies of a CCLME thermal front revealed elevated abundances of gelatinous zooplankton (McClatchie et al., 2012). A growing number of studies are underscoring the importance of fronts to vertebrate species and motivating discussions around designating such habitats as priority conservation areas (Scales et al., 2014).

3.4.2. Water-column occupation in fronts

The association of an individual *M. mola* with upwelling fronts in the southern CCLME (Section 3.4.1) may be due to either (1) passive entrainment into frontal circulation jets while the fish resided near the surface, or (2) active use of frontal environments for a benefit, such as favorable foraging conditions. Fish depth occupation supports the latter explanation (Fig. 6). When the fish was tracked in these frontal environments, it exhibited extensive use of the upper water column, ranging from 125 m to 520 m (Table 3). The individual's activity outside of fronts cannot be compared to activity within fronts because all available synoptic case studies occurred within frontal zones (Fig. 5). When tag

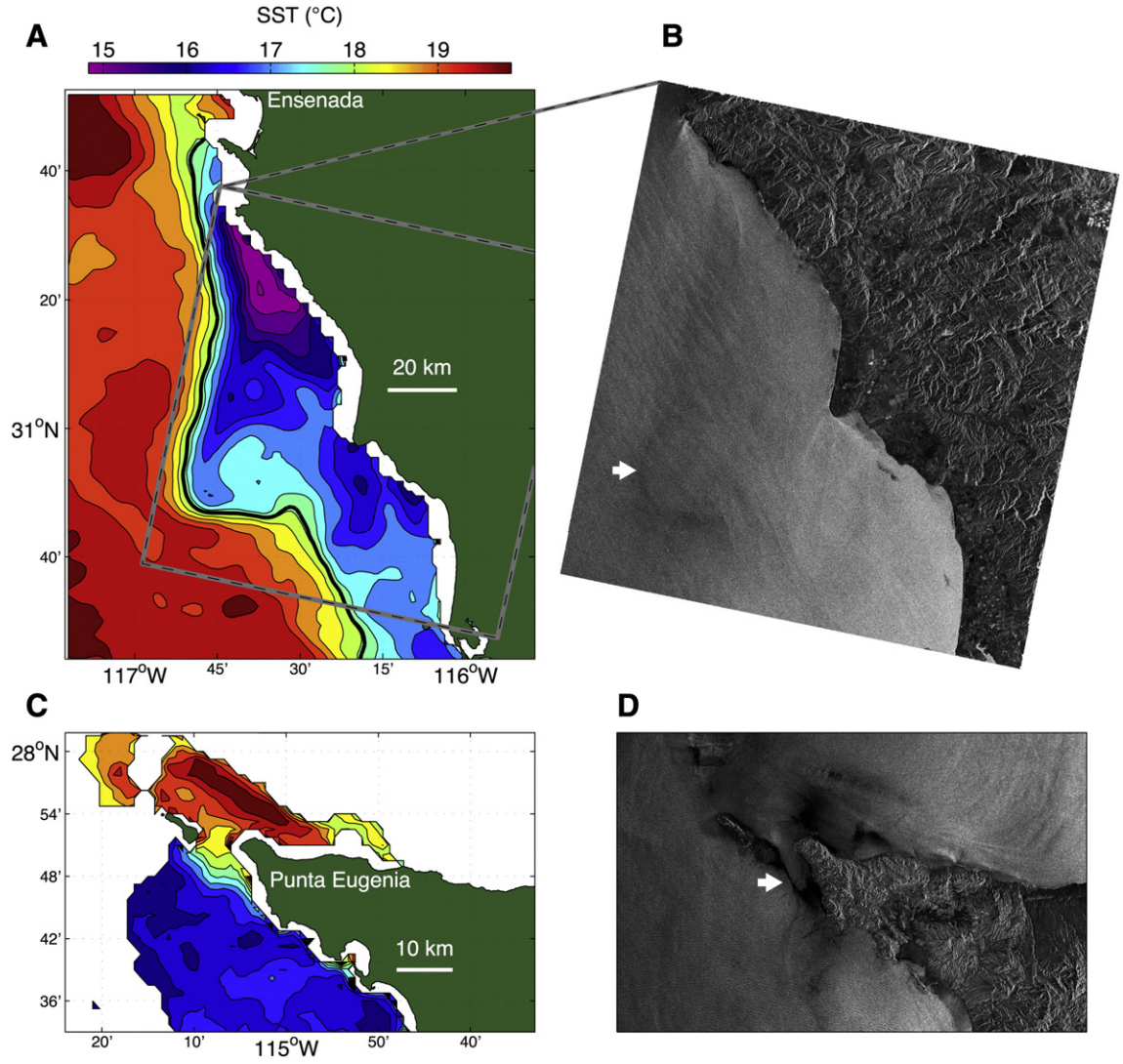

Fig. 7. Convergence in upwelling fronts. (A) AVHRR SST image from September 3, 2010 22:08 UTC approximately one week before the fish transited the region (Fig. 5C, note similar upwelling patterns in this region on September 3 and September 10). (B) ENVISAT synthetic aperture radar (SAR) image within this region from September 3, 2010 17:53 UTC. The arrow identifies a dark band (lower scattering, i.e., smoother ocean surface of a slick) with a similar scale, shape and orientation as the upwelling filament. (C) AVHRR SST image from September 16, 2010 17:43 UTC, approximately one month before the fish transited the region (Fig. 5F–G). (D) ENVISAT SAR image within this region from September 16, 2010 17:45 UTC. The white arrow identifies a dark band in the thermal front, again indicating surface convergence.

data were of sufficient temporal resolution, diel vertical migration (DVM) was evident. Observations of DVM were clearly evidenced over two time periods: (1) between ~10 m (nighttime) and 40 m (daytime) during September 1–4 (Fig. 6B), shortly after the fish was first associated with a front (Fig. 5B), and (2) between ~20 m (nighttime) and 200 m (daytime) during September 20–24 (Fig. 6B, C), during and following occupation in a frontal zone furthest offshore (Fig. 5D). Considering all remote sensing case studies, DVM was evident in depth and/or temperature data for cases c, d, g and i (Figs. 5, 6).

3.4.3. Frontal convergence zones

The observed association of sunfish 89297 with upwelling fronts (Fig. 5) motivated a more detailed investigation of the nature of this habitat. Combined SAR and SST coverage during the tag tracking period permitted examination of two slicks in frontal zones. The first was from the northern region of the fish track on September 3 (Fig. 7A, B), approximately one week before the fish transited the region (Fig. 5C). At that time, a coastal upwelling plume extended ~50 km from the coast near 31°N and was associated with strong thermal gradients (Fig. 7A). A SAR image acquired approximately 4 h before the SST image revealed a dark band having similar location and orientation as the upwelling front (arrow in Fig. 7B). Dark bands indicate slicks typically associated with convergence zones (Holt, 2004; Ryan et al., 2010). Although advection during the hours between the SAR and SST images precluded exact alignment of features in the SST and SAR images, the similarities of the thermal and surface roughness features support the interpretation of a convergent thermal front. The second slick was from the southern region of the track during mid-September (Fig. 7C, D), approximately one month before the fish transited the region (Fig. 5G). Nearly simultaneous SST and SAR images indicated a strong thermal front associated with coastal upwelling and an intense narrow slick in the frontal zone west of Punta Eugenia, Baja California (Fig. 7C, D).

The convergent circulation indicated by these two slicks has both physical and biological implications. When prey species swim upward against the downwelling flow in a convergence, their populations can accumulate (Franks, 1992). This mechanism can create favorable foraging habitats for predators such as *M. mola*.

3.4.4. Forage species in relation to fronts

Zooplankton sampling and environmental conditions within the southern region of the fish's (89297) migration allows further exploration of the strong association between *M. mola* and upwelling fronts. The two highest zooplankton biovolumes were sampled near the coast (Fig. 8, stations near 26.5°N and 28°N), where the sunfish spent half of the total two-month tracking period. Zooplankton biovolume at both stations was dominated by salps, a known prey item for *M. mola* particularly those >1 m (Cardona et al., 2012; Harrod et al., 2013; Nakamura and Sato, 2014; Syvaranta et al., 2012). In contrast, a near-coastal station sampled between these two high-abundance stations showed low biovolume (Fig. 8, station near 26.9°N). This difference in zooplankton biovolume was further related to frontal conditions. At the two near-coastal stations with high zooplankton biovolume, sampling occurred toward the warm side of strong thermal fronts (Fig. 9A, B, D). At the near-coastal station with low zooplankton biovolume, sampling occurred toward the cold side of a weaker thermal front (Fig. 9A, C). Although the zooplankton and environmental sampling were conducted on a prescribed grid, and thus not specifically designed to examine relationships between zooplankton and fronts, the available data

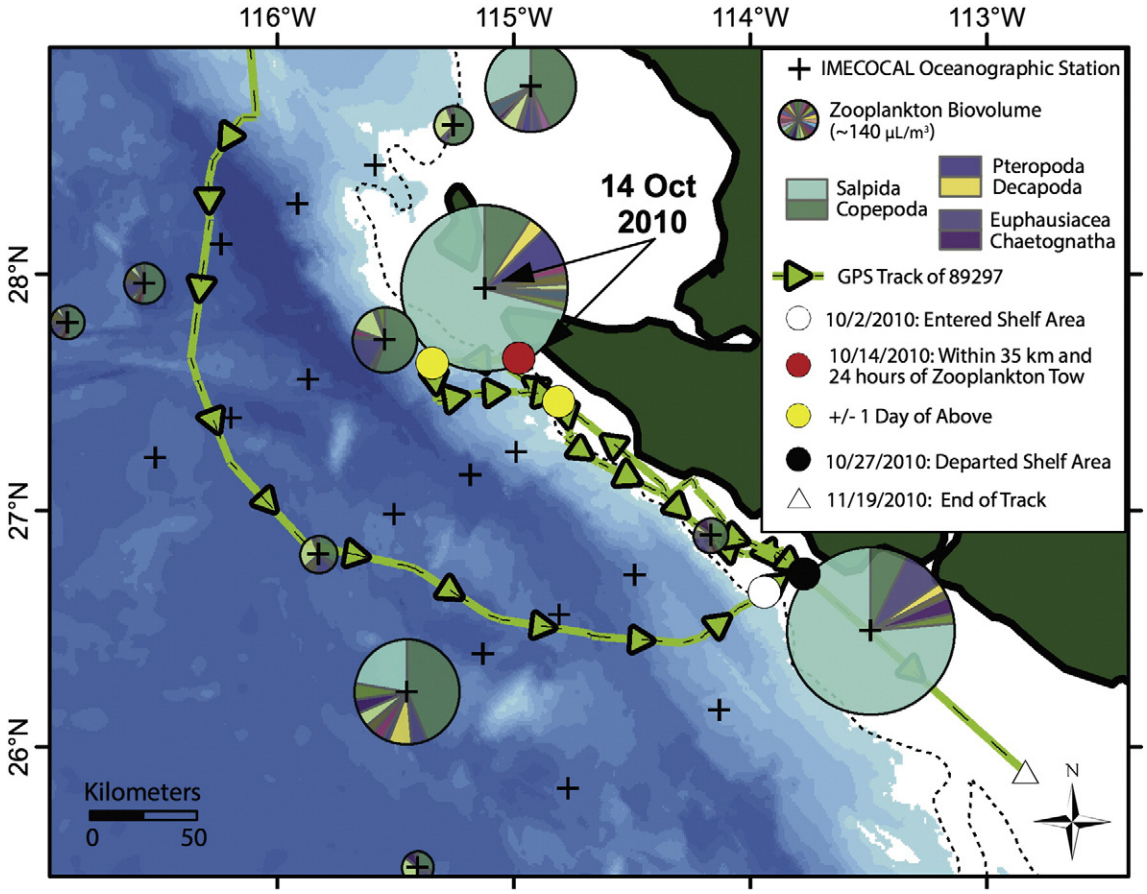

Fig. 8. Zooplankton abundance in the region occupied for nearly one month by the largest tagged *M. mola* (2 m TL, tag 89297, green line). Plus signs (+) mark the locations of ship hydrocast stations; zooplankton was sampled at a subset of stations (pie charts). The pie chart colors in the legend identify the dominant taxa in the two net tows having the greatest abundance. The dashed line is the 200 m isobath, representing the shelf break.

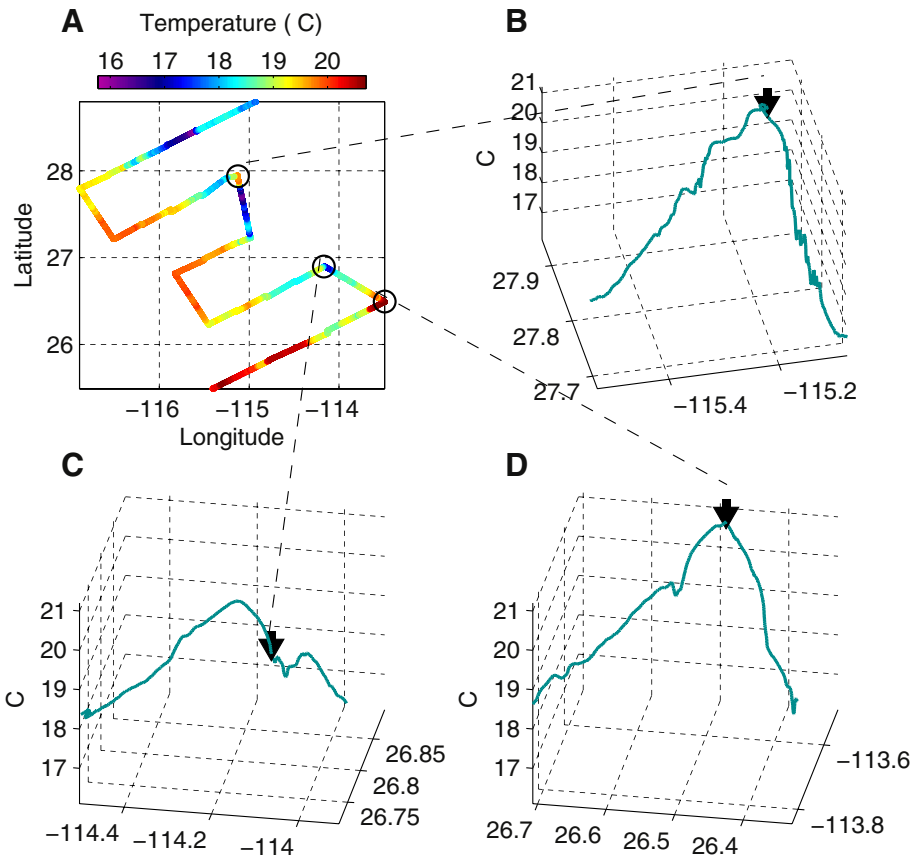

Fig. 9. Relationships between zooplankton abundance and fronts. (A) Near-surface (2 m) temperature along the ship track indicated by the + symbols in Fig. 8, which progressed from north to south during October 12–17, 2010. (B–D) Temperature gradient plots representing the relationship between fronts and zooplankton biomass at the three nearshore stations (pie charts in Fig. 8); arrows define the location and temperature of the zooplankton sampling station.

support the interpretation that zooplankton biovolume was greater on the warm side of strong thermal fronts. Studies in the northeastern Atlantic report finding *M. mola* on the warm stratified side of fronts, both tidal and seasonal (Sims and Southall, 2002). The same may hold true for *M. mola* in the southern CCLME.

3.4.5. Swimming speeds

The high accuracy and temporal intervals of the Fastloc GPS tag data provided the opportunity to examine possible speed bursts of the large (2 m TL) Fastloc tagged individual. Two unusually high speeds were detected during very short bursts. Each was based on GPS locations derived from 6 satellites at one location and 4 satellites at the other. Recent examination of Fastloc GPS accuracy shows that for positions calculated using 6 GPS satellites, 50% of locations were within 18 m, and 95% were within 70 m of the true position (Dujon et al., 2014). Accuracy based on 4 GPS satellites was lower, with 50% of locations within 36 m, and 95% were within 724 m of the true position. The speed estimate for the first burst was 6.6 m s^{-1} during a 370 s interval with a corresponding error of ±0.15 (50% confidence) or ±2.1 (95% confidence). The speed estimate for the second burst was 2.2 m s^{-1} during a 342 s interval with a corresponding error of ±0.22 m s^{-1} (50% confidence) or ±3.2 m s^{-1} (95% confidence). Given this positional uncertainty, we interpret the highest speed calculation, 6.6 ± 2.1 m s^{-1}, with 95% confidence, as a reliable measure of a speed burst and not an outlier due to sampling or reporting error. Further, even with contribution to speed over ground from a strong flow in the California Current of ~0.5 m s^{-1} (Lynn and Simpson, 1987), this speed measurement remains anomalous. The uncertainty in the second measurement exceeds the speed estimate at the 95% confidence level and thus cannot be reliably interpreted as a speed burst. Nakamura and Sato (2014) report a maximum burst speed of ~2.1 m s^{-1} for a smaller individual (1 m TL). Our estimate for maximum speed burst (6.6 m s^{-1}) exceeds this by a factor of 3.

4. Conclusions

M. mola satellite telemetry studies in the southern CCLME between 2003 and 2010 show that the species uses coastal ocean margins and engages in seasonal latitudinal movements extending between Southern California and central Baja California, Mexico. Satellite and ship data coupled with a high accuracy GPS track suggest that *M. mola* consistently occupy frontal zones where potential prey species such as salps may be concentrated. Further, ship measurements of oxygen profiles show that a *M. mola* occupying near-coastal water likely spent time in hypoxic conditions. This observation motivates further physiological studies of the species and tag-based oxygen measurements.

Studying individual *M. mola* offers valuable insight into the species' natural history and behavior in the eastern Pacific, yet important gaps still remain in our understanding of the species' population ecology. Ongoing genetic surveys of the population coupled with citizen science observations (e.g. oceansunfish.org) and aerial and shipboard surveys that record ocean sunfish sightings opportunistically (e.g. Barlow and Forney, 2007; Benson et al., 2007) can help fill gaps. In the western Atlantic, such opportunistic ocean sunfish observations have been used to estimate summer abundances and establish a baseline for population status assessments (Kenney, 1996). Similar work could be used to assess population status for the eastern Pacific *M. mola* population. Gaps also remain in our understanding of ocean sunfish recruitment. Despite high fecundity, with an estimated 300 million eggs reported for a 1.2 m TL individual (Schmidt, 1921), no data exist on *M. mola* reproductive

habits in the CCLME and beyond. While schools of small sunfish (20–30 cm TL) have been reported in the SCB and further north (www.oceansunfish.org) nothing is known regarding spawning locations, or larval recruitment into regional populations and the factors that control it.

Information on habitat preferences and vertical distribution may be of use to fisheries managers for reducing bycatch in DGN fisheries especially if efforts to move toward dynamic ocean management are successful. Additional long-term studies of more individuals encompassing a larger size range and tag deployments from Mexico to north of the SCB will allow further exploration of how this species uses the full extent of the CCLME. The cosmopolitan distribution of *M. mola*, its large size and capacity to carry instruments, coupled with its habit of surfacing provide a unique opportunity to compare behaviors and movements in vastly different ecosystems worldwide.

Acknowledgments

This work was funded by a grant to T.M.T. from the National Geographic Committee for Research and Exploration grant #7369-02 J.P.R. was supported by the David and Lucile Packard Foundation. The IMECOCAL Mexican oceanographic program is funded by CICESE project #625114 and CONACYT project #129140. The Census of Marine Life, Tagging of Pacific Predators TOPP and the Monterey Bay Aquarium Foundation provided additional tag support. Special thanks to: J.D.R. Houghton, B. Robison, R. Vetter and two anonymous reviewers for comments on an earlier version of the manuscript; Dan Lawson for supplying information on the California offshore drift gillnet fishery; Mike Johnson for photos and tagging assistance; Eddie Kisfaludy, Daren Maurer, Suzanne Kohin and NOAA staff, the Rosenthal family, Thomas Behrend, Christina Karliczek from Blue Planet Film and the Block lab for additional tag assistance; M. Salisbury for help in the preparation of Fig. 2 and Emily Nixon for assembling references. This paper is dedicated to the memory of Dave Foley, a great satellite oceanographer and friend. **[SS]**

References

Apel, J.R., 2004. Oceanic internal waves and solutions. In: Apel, J.R., Jackson, C.R. (Eds.), Synthetic Aperture Radar Marine User's Manual. NOAA, Washington, D.C., pp. 189–206.

Barlow, J., Forney, K.A., 2007. Abundance and density of cetaceans in the California Current ecosystem. Fish. Bull. 105 (4), 509–526.

Bass, A.L., Dewar, H., Thys, T., Streelman, J.T., Karl, S.A., 2005. Evolutionary divergence among lineages of the ocean sunfish family, Molidae (Tetraodontiformes). Mar. Biol. 148 (2), 405–414.

Belkin, I.M., Hunt Jr., G.L., Hazen, E.L., Zamon, J.E., Schick, R., Prieto, R., Brodziak, J., Hare, J., Teo, S.L.H., Thorne, L., Bailey, H., Itoh, S., Munk, P., Musyl, M.K., Willis, J.K., Zhang, W., 2014. Fronts, fish, and predators. Deep-Sea Res. II Top. Stud. Oceanogr. 107, 1–2.

Benson, S.R., Forney, K.A., Harvey, J.T., Carretta, J.V., Dutton, P.H., 2007. Abundance, distribution and habitat of leatherback turtles (*Dermochelys coriacea*) off California, 1990–2003. Fish. Bull. 105, 337–347.

Block, B.A., Jonsen, I.D., Jorgensen, S.J., Winship, et al., 2011. Tracking apex marine predator movements in a dynamic ocean. Nature 475, 86–90.

Bograd, S.J., Castro, C.G., Di Lorenzo, E., Palacios, D.M., Bailey, H., Gilly, W., Chavez, F.P., 2008. Oxygen declines and the shoaling of the hypoxic boundary in the California Current. Geophys. Res. Lett. 35 (12). http://dx.doi.org/10.1029/2008GL034185.

Brill, R.W., 1994. A review of temperature and oxygen tolerance studies of tuna pertinent to fisheries oceanography, movement models and stock assessments. Fish. Oceanogr. 3 (3), 204–216.

Cardona, L., Álvarez de Quevedo, I., Borrell, A., Aguilar, A., 2012. Massive consumption of gelatinous plankton by Mediterranean apex predators. PLoS One 7 (3), e31329. http://dx.doi.org/10.1371/journal.pone.0031329.

Cartamil, D.P., Lowe, C.G., 2004. Diel movement patterns of ocean sunfish *Mola mola* off southern California. Mar. Ecol. Prog. Ser. 266, 245–253.

Carwardine, M., 1995. The Guinness Book of Animal Records. Guinness Publishing, Middlesex, UK.

Costa, D.P., Breed, G.A., Robinson, P.W., 2012. New insights into pelagic migrations: implications for ecology and conservation. Annu. Rev. Ecol. Evol. Syst. 43, 73–96.

Davis, J.C., 1975. Minimal dissolved oxygen requirements of aquatic life with emphasis on Canadian species: a review. J. Fish. Res. Board Can. 32 (12), 2295–2332.

Dewar, H., Thys, T., Teo, S.L.H., Farwell, C., O'Sullivan, J., Tobayama, T., Soichi, M., Nakatsubo, T., Kondo, Y., Okada, Y., Lindsay, D.J., Hays, G.C., Walli, A., Weng, K., Streelman, J.T., Karl, S.A., 2010. Satellite tracking the world's largest jelly predator, the ocean sunfish, *Mola mola*, in the Western Pacific. J. Exp. Mar. Biol. Ecol. 393 (1), 32–42.

Dewar, H., Prince, E., Musyl, M.K., Brill, R.W., Sepulveda, C., Lou, J., Foley, D., Orbesen, E.S., Domeier, M.L., Nasby-Lucas, N., Snodgrass, D., Laurs, R.M., Block, B.A., McNaughton, L.A., 2011. Movements and behaviors of swordfish in the Atlantic and Pacific oceans examined using pop-up satellite archival tags. Fish. Oceanogr. 20 (3), 219–241.

Dujon, A.M., Lindstrom, T., Hays, G.C., 2014. The accuracy of Fastloc-GPS locations and implications for animal tracking. Methods Ecol. Evol. 5 (11), 1162–1169. http://dx.doi.org/10.1111/2041-210X.12286.

Etnoyer, P., Canny, D., Mate, B., Morgan, L., Ortega-Ortiz, J., 2006. Sea-surface temperature gradients across blue whale and sea turtle foraging trajectories off the Baja California Peninsula, Mexico. Deep-Sea Research II. Top. Oceanogr. 53 (3), 340–358.

Fiedler, P.C., Bernard, H.J., 1987. Tuna aggregation and feeding near fronts observed in satellite imagery. Cont. Shelf Res. 7 (8), 871–881.

Franks, P.J.S., 1992. Sink or swim: accumulation of biomass at fronts. Mar. Ecol. Prog. Ser. 82 (1), 1–12.

Hakel, M., Stewart, J.D., 2002. First fossil Molidae (Actinopterygii: Tetraodontiformes) in Western North America. J. Paleontol. 22, 62A.

Harrod, C., Syväranta, J., Kubicek, L., Cappanera, V., Houghton, J.D.R., 2013. Reply to Logan and Dodge: stable isotopes challenge the perception of ocean sunfish *Mola mola* as obligate jellyfish predators. J. Fish Biol. 82 (1), 10–16.

Hays, G.C., Broderick, A.C., Godley, B.J., Luschi, P., Nichols, W.J., 2003. Satellite telemetry suggests high levels of fishing-induced mortality in marine turtles. Mar. Ecol. Prog. Ser. 262, 305–309.

Hays, G., Farquhar, M., Luschi, P., Teo, S., Thys, T., 2009. Vertical niche overlap by two ocean giants with similar diets: ocean sunfish and leatherback turtles. J. Exp. Mar. Biol. Ecol. 370 (1), 134–143.

Hofmann, G.E., Evans, T.G., Kelly, M.W., Padilla-Gamiño, J.L., Blanchette, C.A., Washburn, L., Chan, F., McManus, M.A., Menge, B.A., Gaylord, B., Hill, T.M., Sanford, E., LaVigne, M., Rose, J.M., Kapsenberg, L., Dutton, J.M., 2014. Exploring local adaptation and the ocean acidification seascape — studies in the California Current Large Marine Ecosystem. Biogeosciences 11, 1053–1064.

Holt, B., 2004. SAR imaging of the ocean surface. In: Jackson, C.R., Apel, J.R. (Eds.), in Synthetic Aperture Radar Marine User's Manual. NOAA, Washington, D. C., pp. 25–80.

Hoolihan, J.P., Luo, J., Abascal, F.J., Campana, S.E., De Metrio, G., Dewar, H., Domeier, M.L., Howey, L.A., Lutcavage, M.E., Musyl, M.K., Neilson, J.D., Orbesen, E.S., Prince, E.D., Rooker, J.R., 2011. Evaluating post-release behaviour modification in large pelagic fish deployed with pop-up satellite archival tags. ICES J. Mar. Sci. 68 (5), 880–889.

Houghton, J.D.R., Doyle, T.K., Davenport, J., Wilson, R.P., Hays, G.C., 2008. The role of infrequent and extraordinary deep dives in leatherback turtles (*Dermochelys coriacea*). J. Exp. Biol. 211, 2566–2575. http://dx.doi.org/10.1242/jeb.020065.

Joslin, T.L., 2012. Early Holocene prehistoric fishing strategies at CA-SBA-139, Western Santa Barbara County, California. Report Prepared for Central Coast Archeological Research Consultants.

Kenney, R.D., 1996. Preliminary assessment of competition for prey between leatherback sea turtles and ocean sunfish in northeast shelf waters. In: Keinath, J.A., Bernard, D.E., Musick, J.A., Bell, B.A. (Eds.), Proceedings of the 15th Annual Symposium on Sea Turtle Biology and Conservation. National Marine Fisheries Service, Miami, FL, pp. 144–147.

Lam, C.H., Nielsen, A., Sibert, J.R., 2010. Incorporating sea-surface temperature to the light-based geolocation model TrackIt. Mar. Ecol. Prog. Ser. 419, 71–84.

Lavaniegos, B.E., Jimenez-Perez, L.C., Gaxiola-Castro, G., 2002. Plankton response to El Nino 1997–1998 and La Nina 1999 in the southern region of the California Current. Prog. Oceanogr. 54 (1), 33–58.

Lynn, R.L., Simpson, J.J., 1987. The California Current System: the seasonal variability of its physical characteristics. J. Geophys. Res. 92, 12,947–12,966.

Lyzenga, D.R., Marmorino, G.O., Johannessen, J.A., 2004. Ocean currents and current gradients. In: Jackson, C.R., Apel, J.R. (Eds.), Synthetic Aperture Radar Marine User's Manual. NOAA, Washington, D.C., pp. 207–220.

McClatchie, S.R., Goericke, R., Cosgrove, R., Auad, G., Vetter, R., 2010. Oxygen in the Southern California Bight: multidecadal trends and implications for demersal fisheries. Geophys. Res. Lett. 37 (19). http://dx.doi.org/10.1029/2010GL044497.

McClatchie, S., Cowen, R., Nieto, K., Greer, A., Luo, J.Y., Guigand, C., Demer, D., Griffith, D., Rudnick, D., 2012. Resolution of fine biological structure including small Narcomedusae across a front in the Southern California Bight. J. Geophys. Res. Oceans 117, C4. http://dx.doi.org/10.1029/2011JC007565.

Nakamura, I., Sato, K., 2014. Ontogenetic shift in foraging habit of ocean sunfish *Mola mola* from dietary and behavioral studies. Mar. Biol. 161 (6), 1263–1273.

Nakamura, I., Goto, Y., Sato, K., 2015. Ocean sunfish rewarm at the surface after deep excursions to forage for siphonophores. J. Anim. Ecol. http://dx.doi.org/10.1111/1365-2656.12346.

Nielsen, A., Sibert, J.R., 2007. State-space model for light-based tracking of marine animals. Can. J. Fish. Aquat. Sci. 64 (8), 1055–1068.

Nielsen, A., Bigelow, K.A., Musyl, M.K., Sibert, J.R., 2006. Improving light-based geolocation by including sea surface temperature. Fish. Oceanogr. 15 (4), 314–325.

NOAA, 2014. Online:, http://www.nwfsc.noaa.gov/news/features/food_chain/index.cfm accessed January 2015.

Parsons, T.R., Takahashi, M., Hargrave, B., 1984. Biological Oceanographic Processes. 3rd ed. Pergamon Press, Oxford UK (332 pp.).

Peckham, S., Diaz, D., Walli, A., Ruiz, G., Crowder, L., 2007. Small-scale fisheries bycatch jeopardizes endangered Pacific loggerhead turtles. PLoS One 2 (10), e1041. http://dx.doi.org/10.1371/journal.pone.0001041.

Petersen, S., 2005. Initial bycatch assessment: South Africa's domestic longline fishery, 2000–2003. Domestic Pelagic Longline Fishery: Bycatch Report 2000–2003. BirdLife South Africa (45 pp.).

Petersen, S., McDonell, Z., 2007. A bycatch assessment of the Cape horse mackerel, *Trachurus trachurus capensis*, mid-water trawl fishery of South Africa. Birdlife/WWF Responsible Fisheries Programme Report 2002–2003 (30 pp.).

Pope, E., Hays, G., Thys, T., Doyle, T., Sims, D., Queiroz, N., Hobson, V., Kubicek, L., Houghton, J.D.R., 2010. The biology and ecology of the ocean sunfish *Mola mola*: a review of current knowledge and future research perspectives. Rev. Fish Biol. Fish. 20 (4), 471–487. http://dx.doi.org/10.1007/s11160-009-9155-9.

Porcasi, J.F., Andrews, S.L., 2001. Evidence for a prehistoric *Mola mola* fishery on the Southern California coast. J. Calif. Great Basin Anthropol. 23 (1), 51–66.

Potter, I.F., Howell, W.H., 2011. Vertical movements and behavior of the ocean sunfish, *Mola mola*, in the Northwest Atlantic. J. Exp. Mar. Biol. Ecol. 396 (2), 138–146.

Potter, I.F., Galuardi, B., Howell, W.H., 2011. Horizontal movement of ocean sunfish, *Mola mola*, in the Northwest Atlantic. Mar. Biol. 158 (3), 531–540.

R Development Core Team, 2013. R: A Language and Environment for Statistical Computing. R Foundation for Statistical Computing, Vienna (www.r-project.org/. Retrieved 23 July 2013).

Roach, J., 2003. World's Heaviest Bony Fish Discovered? National Geographic (news.nationalgeographic.com/news/2003/05/0513_030513_sunfish.html. accessed 23 July 2013)

Ryan, J.P., Fischer, A.M., Kudela, R.M., McManus, M.A., Myers, J.S., Paduan, J.D., Ruhsam, C.M., Woodson, C.B., Zhang, Y., 2010. Recurrent frontal slicks of a coastal ocean upwelling shadow. J. Geophys. Res. Oceans 115, C12. http://dx.doi.org/10.1029/2010JC006398.

Ryan, J.P., Dierssen, H.M., Kudela, R.M., Scholin, C.A., Johnson, K.S., Sullivan, J.M., Fischer, A.M., Rienecker, E.V., McEnaney, P.R., Chavez, F.P., 2005. Coastal ocean physics and red tides, an example from Monterey Bay, California. Oceanography 18, 246–255.

Ryan, J.P., McManus, M.A., Paduan, J.D., Chavez, F.P., 2008. Phytoplankton thin layers within coastal upwelling system fronts. Mar. Ecol. Prog. Ser. 354, 21–34. http://dx.doi.org/10.3354/meps07222.

Sawai, E., Yamanoue, Y., Yoshita, Y., Sakai, Y., Hashimoto, H., 2011. Seasonal occurrence patterns of Mola sunfishes (*Mola* spp. A and B; Molidae) in waters off the Sanriku region, eastern Japan. Japn. J. Ichthyol. 58 (2), 181–187.

Scales, K.L., Miller, P.I., Hawkes, L.A., Ingram, S.N., Sims, D.W., Votier, S.C., 2014. On the front line: frontal zones as priority at-sea conservation areas from mobile marine vertebrates. J. Appl. Ecol. 51 (6), 1575–1583. http://dx.doi.org/10.1111/1365-2664.12330.

Schaefer, K., Fuller, D., Block, B., 2007. Movements, behavior, and habitat utilization of yellowfin tuna (*Thunnus albacares*) in the northeastern Pacific Ocean, ascertained through archival tag data. Mar. Biol. 152 (3), 503–525.

Schmidt, J., 1921. New studies of sun-fishes made during the "Dana" Expedition, 1920. Nature 107, 76–79.

Silvani, L., Gazo, M., Aguilar, A., 1999. Spanish driftnet fishing and incidental catches in the western Mediterranean. Biol. Conserv. 90 (1), 79–85.

Sims, D.W., Southall, E.J., 2002. Occurrence of ocean sunfish, *Mola mola*, near fronts in the western English Channel. J. Mar. Biol. Assoc. UK 82 (5), 927–928.

Sims, D.W., Queiroz, N., Doyle, T.K., Houghton, J.D.R., Hayes, G., 2009a. Satellite tracking of the world's largest bony fish, the ocean sunfish (*Mola mola*) in the North East Atlantic. J. Exp. Mar. Biol. Ecol. 370 (1), 127–133.

Sims, D.W., Queiroz, N., Humphries, N., Lima, F., Hays, G., 2009b. Long-term GPS tracking of ocean sunfish, *Mola mola*, offers a new direction in fish monitoring. PLoS One 4 (10), e7351. http://dx.doi.org/10.1371/ journal.pone.0007351.

Stramma, L., Schmidtko, S., Levin, L., Johnson, G., 2010. Ocean oxygen minima expansions and their biological impacts. Deep-Sea Res. I Oceanogr. Res. Pap. 57 (4), 587–595.

Syvaranta, J., Harrod, C., Kubicek, L., Cappanera, V., Houghton, J.D.R., 2012. Stable isotopes challenge the perception of ocean sunfish *Mola mola* as obligate jellyfish predators. J. Fish Biol. 80 (1), 225–231.

Tudela, S., Kai Kai, A., Maynou, F., El Andalossi, M., Guglielmi, P., 2005. Driftnet fishing and biodiversity conservation: the case study of the large-scale Moroccan driftnet fleet operating in the Alboran Sea (SW Mediterranean). Biol. Conserv. 121 (1), 65–78.

Tynan, C.T., Ainley, D.G., Barth, J.A., Cowles, T.J., Pierce, S.D., Spear, L.B., 2005. Cetacean distributions relative to ocean processes in the northern California Current System. Deep-Sea Res. II Top. Stud. Oceanogr. 52 (1), 145–167.

Watanabe, Y., Sato, K., 2008. Functional dorsoventral symmetry in relation to lift-based swimming in the ocean sunfish Mola mola. PLoS One 3 e3446.

Wingfield, D.K., Peckham, S.H., Foley, D.G., Palacios, D.M., Lavaniegos, B.E., Durazo, R., Nichols, W.J., Croll, D.A., Bograd, S.J., 2011. The making of a productivity hotspot in the coastal ocean. PLoS One 6 (11), e27874.

Wolf, S., Sydeman, W., Hipfner, J., Abraham, C., Tershy, B., 2009. Range-wide reproductive consequences of ocean climate variability for the seabird, Cassin's Auklet. Ecology 90 (3), 742–753.

Yoshita, Y., Yamanoue, Y., Sagara, K., Nishibori, M., Kuniyoshi, H., Umino, T., Sakai, Y., Hashimoto, H., Gushima, K., 2009. Phylogenetic relationship of two Mola sunfishes (Tetraodontiformes: Molidae) occurring around the coast of Japan, with notes on their geographical distribution and morphological characteristics. Ichthyol. Res. 56 (3), 232–244. http://dx.doi.org/10.1007/s10228-008-0089-3.

Further Reading

www.argos-system.org/manual/3-location/34_location_classes.html (Retrieved January 2, 2015).

www.westcoast.fisheries.noaa.gov/fisheries/wc_oberserver_program_info/data_summ_report_sw_observer_fish.html (Retrieved January 2 2015).